scientific reports

Check for updates

OPEN

The histone H3K9 methyltransferase G9a regulates tendon formation during development

Satoshi Wada[1,2,3,6], Hisashi Ideno[1,6], Kazuhisa Nakashima[1], Koichiro Komatsu[1], Noboru Demura[2], Hiroshi Tomonari[3], Hiroshi Kimura[4], Makoto Tachibana[5] & Akira Nifuji[1]✉

G9a is a histone methyltransferase that catalyzes the methylation of histone 3 lysine 9 (H3K9), which is involved in the regulation of gene expression. We had previously reported that G9a is expressed in developing tendons in vivo and in vitro and that G9a-deficient tenocytes show impaired proliferation and differentiation in vitro. In this study, we investigated the functions of G9a in tendon development in vivo by using G9a conditional knockout (*G9a* cKO) mice. We crossed *Sox9*$^{Cre/+}$ mice with *G9a*$^{fl/fl}$ mice to generate *G9a*$^{fl/fl}$; *Sox9*$^{Cre/+}$ mice. The *G9a* cKO mice showed hypoplastic tendon formation at 3 weeks of age. Bromodeoxyuridine labeling on embryonic day 16.5 (E16.5) revealed decreased cell proliferation in the tenocytes of *G9a* cKO mice. Immunohistochemical analysis revealed decreased expression levels of G9a and its substrate, H3K9me2, in the vertebral tendons of *G9a* cKO mice. The tendon tissue of the vertebrae and limbs of *G9a* cKO mice showed reduced expression of a tendon marker, *tenomodulin* (*Tnmd*), and *col1a1* genes, suggesting that tenocyte differentiation was suppressed. Overexpression of G9a resulted in enhancement of *Tnmd* and *col1a1* expression in tenocytes in vitro. These results suggest that G9a regulates the proliferation and differentiation of tendon progenitor cells during tendon development. Thus, our results suggest that G9a plays an essential role in tendon development.

Keywords Epigenetics, Histone modification, Tenocytes, Proliferation, Cell differentiation

Abbreviations

H3K9	Histone H3 lysine 9
H3K9MTase	H3K9 methyltransferase
H3K9me1	monomethylation at Lys 9 of histone H3
H3K9me2	dimethylation at Lys 9 of histone H3

Epigenetic modifications play important roles in development and differentiation by regulating cell lineage-specific genes. Epigenetic modifications include post-translational modifications of histones, which regulate nuclear organization, chromatin structure, and gene expression[1]. Among histone modifications, methylation of histone 3 lysine 9 (H3K9) is a crucial modification that affects cell differentiation[2]. The methylated forms of H3K9, namely, H3K9me1, H3K9me2, and H3K9me3, are heterochromatin-associated histone modifications that play a role in genome compartmentalization[3]. Histone methyltransferases determine the methylated state of H3K9[4]. One of these histone methyltransferases, G9a (also known as Ehmt2), catalyzes the mono- and dimethylation of H3K9 (H3K9me1 and H3K9me2)[5]. G9a contributes to transcriptional silencing via heterochromatin formation[6–8]. In vivo study showed that *G9a* KO embryo died around embryonic day 8 (E8), indicating that it is indispensable for early mouse development[9]. G9a suppresses germline-specific genes through DNA methylation

[1]Department of Pharmacology, School of Dental Medicine, Tsurumi University, Yokohama, Kanagawa 230-8501, Japan. [2]Department of Oral and Maxillofacial Surgery, School of Medicine, Kanazawa Medical University, Uchinada, Ishikawa 920-0293, Japan. [3]Department of Orthodontics, School of Dental Medicine, Tsurumi University, Yokohama, Kanagawa 230-8501, Japan. [4]Department of Biological Sciences, Graduate School of Bioscience and Biotechnology, Tokyo Institute of Technology, Yokohama, Kanagawa 226-8501, Japan. [5]Laboratory of Epigenome Dynamics, Graduate School of Frontier Biosciences, Osaka University, Suita, Osaka 565-0871, Japan. [6]These authors contributed equally: Satoshi Wada and Hisashi Ideno. ✉email: nifuji-a@tsurumi-u.ac.jp

during mouse embryogenesis[10]. In mouse oocytes, it regulates chromatin reorganization[11]. G9a also methylates non-histones proteins and regulates various biological processes. In myogenic differentiation, G9a suppresses functions of the myogenic regulatory factor MyoD by directly methylating it at lysine residue[12]. G9a regulates gene expression as a co-activator for nuclear hormone receptors such as estrogen receptor α (ERα), glucocorticoid receptors (GR), or critical transcriptional factor[13–16]. G9a and G9a-like protein (GLP) act as coactivators for a subset of GR target genes and their post-translational methylation are important for coactivator function[16]. G9a dimethylates ERα and functions as an ERα coactivator to affect hormonal target genes in breast cancer cells[17]. In erythroid cells, G9a activates *β maj-globin* gene by stabilizing pre-initiation complex (PIC) formation, and direct G9a -Pol II interaction is involved in this process[18]. We previously reported that G9a is expressed in the growth plate of the skeleton[19], the mesenchyme of tooth germs[20], and tendons[21]. In addition, G9 regulates cranial bone development by activating the function of an osteoblastic transcription factor, Runx2[15]. Thus, G9a plays important biological roles by suppressing or activating gene expression.

Tendons are composed of fibrous connective tissue that connects muscles to bone to transmit the force generated by muscle contraction, thus playing important roles in the locomotor system. During development, tendon progenitor cells are derived from mesenchyme condensation of somite and neural crest. The progenitors express two critical transcription factors, scleraxis (Scx) and SRY-box containing gene 9 (Sox9)[22,23]. Lineage analysis using *Sox9-Cre* showed that *Sox9*-expressing cells differentiate into tendon cells[24,25]. Scx continues to be expressed in tendon progenitors during development, whereas Sox9 expression shifts from the progenitors to chondrocytes and tendon-bone junctional tissues. Differentiation of tendon cells proceeds through production of extracellular matrix (ECM) components, such as type I, III, V, VI, and XII collagens and proteoglycans, including decorin, fibromodulin, and biglycan[26–28]. The expression of these ECM proteins is regulated by tendon-specific transcriptional factors such as Scx, Mohawk (Mkx), and Egr1[29–33]. Recent genome-wide study showed the existence of multiple Scx binding sites of Scx-dependent genes including *tenomodulin* (*Tnmd*), *sine oculis-related homeobox 2* (*Six2*), and *fibromodulin* (*Fmod*)[34]. The functions of the transcriptional factors may be influenced by epigenetic modifiers, including histone methyltransferases. Enhancer of zeste homolog 2 (EZH2) which catalyzes histone H3 lysine (K) 27 methylation, was shown to be essential for early patterning of all musculoskeletal tissues in EZH2 cKO mice by *Prx1-Cre*. When EZH2 was deleted by tendon-specific *Scx-Cre* in the EZH2 cKO mice, formation of tendon collagen matrix was not affected, suggesting that EZH2 is likely to be dispensable for tendon differentiation[35]. We had previously shown that another epigenetic modifier, G9a, is expressed in the early stage of tendon development, and that the expression of tendon-related genes and proliferation are suppressed in G9a-null tenocytes in vitro[21]. However, involvement of G9a in tendon formation in vivo have not yet been investigated.

In this study, we wished to determine roles of G9a in tendon formation in vivo. We generated G9a conditional knockout (*G9a* cKO) mice, in which G9a was deleted from tendon progenitor cells using *Sox9-Cre* as a Cre-mediating gene deletion[24]. We first confirmed that *Sox9-Cre* is functional in the tendon progenitor cells in vivo. We then crossed $G9a^{fl/fl}$ mice with $Sox9^{Cre/+}$ mice to create *G9a* cKO mice. Our results demonstrated that tendon tissue in *G9a* cKO mice is hypoplastic, and that this hypoplasia may be associated with inhibition of cell growth and differentiation during tendon development.

Results

Sox9-Cre is active in the tendon progenitor cells

To investigate G9a function in tendon formation in vivo, we generated tendon-specific *G9a* cKO mice by crossing $G9a^{fl/fl}$ mice with $Sox9^{Cre/+}$ mice expressing Cre under the control of a specific *Sox9* promoter. Tendon progenitor cells are derived from *Sox9*-expressing cells during development. Therefore, we confirmed the localization of tenocytes derived from *Sox9*-expressing cells using $Sox9^{Cre/+}$; *R26R* mice. The vertebral tendon between the lumbar vertebrae at E16.5 showed β-galactosidase (LacZ) staining (Fig. 1A,B). These results indicated that Cre-recombinase driven by the *Sox9* promoter was active in the vertebral tendon tissue.

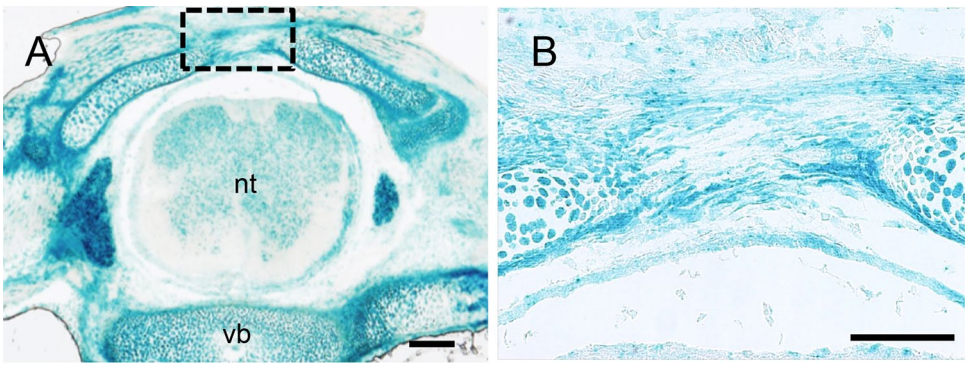

Fig. 1. Analysis of Cre-recombinase expression in tendon tissue using $Sox9^{Cre/+}$; *R26R* mice. (**A**) *LacZ* staining of vertebral tendons in $Sox9^{Cre/+}$; *R26R* mouse embryos at E16.5 (n = 3). Bar = 300 µm. Cre-recombinase driven by the *Sox9* promoter was active in the vertebral tendon tissue at E16.5. (**B**) Enlargement of the boxed area in (**A**). nt, neural tube; vb, vertebral body. Bar = 50 µm.

G9a and H3K9me2 levels decreased in the tendon tissue of *G9a* cKO mice

To investigate levels of G9a and H3K9me2 in the tendon tissue of *G9a* cKO mice, we examined their localization by immunostaining with anti-G9a and H3K9me2 antibodies. G9a expression in the tendon tissues of *G9a* cKO mice was significantly lower than that in control mice (Fig. 2A–D). The percentage of G9a-positive cells was lower in the tendons of *G9a* cKO mice (upper right panel in Fig. 2). Similarly, H3K9me2-positive regions were diminished in the tendon tissue of *G9a* cKO mice (Fig. 2E–H), and the percentage of H3K9me2-positive cells was reduced in the tendon of *G9a* cKO mice (lower right panel in Fig. 2).

Hypoplastic tendon formation in *G9a* cKO mice

Next, we examined tendon formation in *G9a* cKO mice. We previously showed that most of these *G9a* cKO mice died at the time of birth or within 2 days after birth due to defects of the digestive system[36]. A few mice survived after birth and could be analyzed at 3 weeks of age. Visual observation of the tissue revealed that the tendons of the limbs and vertebrae in *G9a* cKO mice were hypoplastic in comparison with those in the control mice at 3 weeks of age (Fig. 3A–F). We then performed histological analysis of the tendon tissue in *G9a* cKO mice. Sections stained with hematoxylin and eosin revealed that the vertebral tendon was thinner in *G9a* cKO

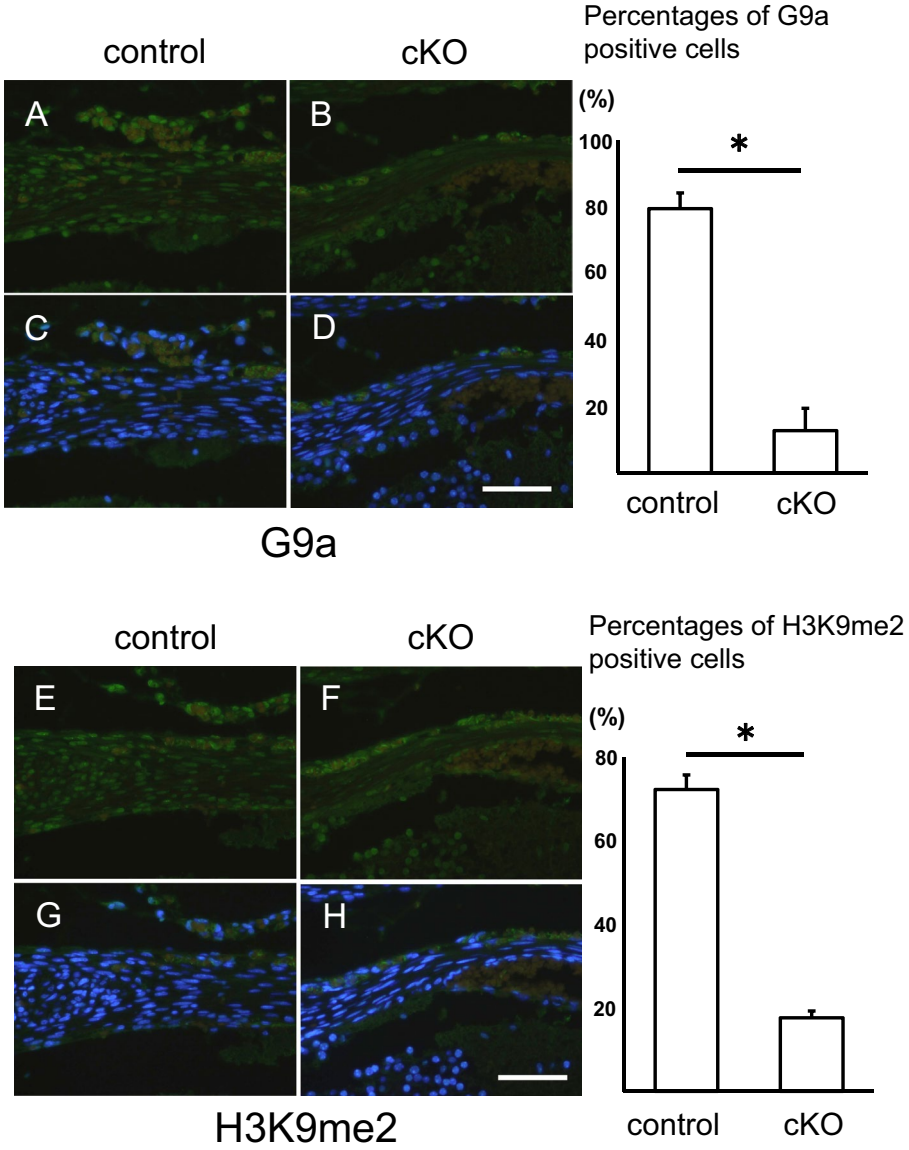

Fig. 2. Decreased G9a and H3K9me2 levels in tendon tissue of *G9a* cKO mice. Immunohistochemical analysis of G9a (**A**–**D**) and H3K9me2 (**E**–**H**) in the vertebral tendon tissue of control ($G9a^{fl/+}$; $Sox9^{Cre/+}$) and *G9a* cKO ($G9a^{fl/fl}$; $Sox9^{Cre/+}$) mouse embryos at E17.5 (control n = 3; cKO n = 3). Immunofluorescent images of staining with anti-G9a (**A** and **B**) and anti-H3K9me2 antibodies (**E** and **F**) (*green*), and merged images of fluorescence signals for immunostaining and nuclear staining with DAPI (*blue*) (**C**, **D**, **G**, and **H**). Bars = 50 µm. The percentages of G9a-positive cells (upper right panel) and H3K9me2 (lower right panel) were shown in control and *G9a* cKO mice (*$p < 0.05$, t-test).

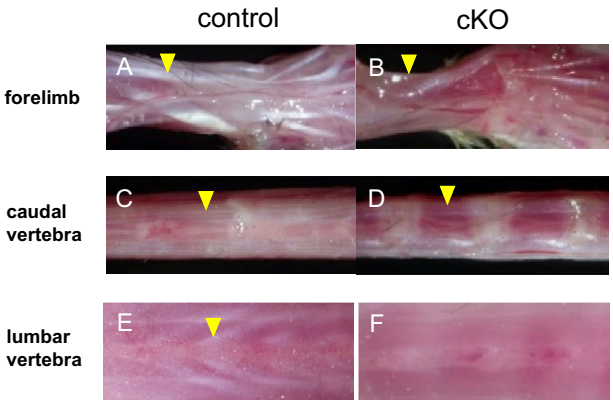

Fig. 3. Hypoplastic tendon formation in *G9a* cKO mice. Tendons of the forelimb (**A** and **B**; yellow arrowheads), caudal vertebrae (**C** and **D**; yellow arrowheads), and lumbar vertebrae (**E** and **F**; yellow arrowheads) in *G9a* cKO mice ($G9a^{fl/fl}$; $Sox9^{Cre/+}$) were compared with those in control mice ($G9a^{fl/+}$; $Sox9^{Cre/+}$) at 3 weeks of age (control n = 3; cKO n = 3). Tendon formation was hypoplastic in all tendons examined.

mice than in the control mice at E16.5 (Fig. 4A–D). Furthermore, Achilles tendon at P0 and masseter tendon at 3 weeks were both hypoplastic in *G9a* cKO mice (Supplemental Fig. 1). Masseter muscle where *Sox9-Cre* was not fully active seems to be unchanged at P21. These results suggest that G9a is required for tendon tissue formation during development.

Loss of G9a inhibits the proliferation of tenocytes in the developing tendon

To investigate the effects of G9a on tendon tissue proliferation, we performed BrdU-labeling experiments by injecting BrdU. Immunohistochemical analysis using the BrdU antibody revealed fewer BrdU-positive cells in the tendon tissue of *G9a* cKO mice (Fig. 5A,B). We confirmed that the percentage of BrdU-positive cells was lower in the vertebral tendon tissue of *G9a* cKO mice at E16.5 (Fig. 5C). To assess cell proliferation, we further examined expression of proliferating cell nuclear antigen (PCNA) in the tendon tissue sections. Immunohistochemical analysis of PCNA revealed that PCNA-positive cells were decreased in vertebral tendon tissue of *G9a* cKO mice at E17.5 (Supplemental Fig. 2). We also examined the effects of G9a deletion on tenocyte apoptosis by using the TUNEL assay (Fig. 5D,E). The TUNEL assay revealed that TUNEL-positive cells were not observed in the tendon tissue of both control and *G9a* KO mice at E16.5. These results suggest that G9a promotes tenocyte proliferation but does not affect apoptosis during tendon formation.

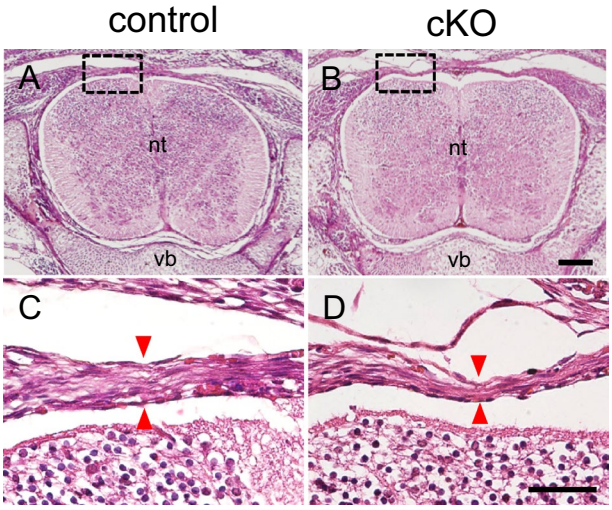

Fig. 4. Decreased width of tendon tissue in *G9a* cKO mice. Histological analysis of vertebral tendons by hematoxylin and eosin staining in control (**A** and **C**, $G9a^{fl/+}$; $Sox9^{Cre/+}$) and *G9a* cKO (**B** and **D**, $G9a^{fl/fl}$; $Sox9^{Cre/+}$) mouse embryos at E16.5 (control n = 3; cKO n = 3). Red arrowheads indicate the width of the vertebral tendon. (**B** and **D**) show enlarged images of the boxed areas in (**A** and **C**), respectively. nt, neural tube; vb, vertebral body. Bar = 300 μm (**A** and **B**), 50 μm (**C** and **D**).

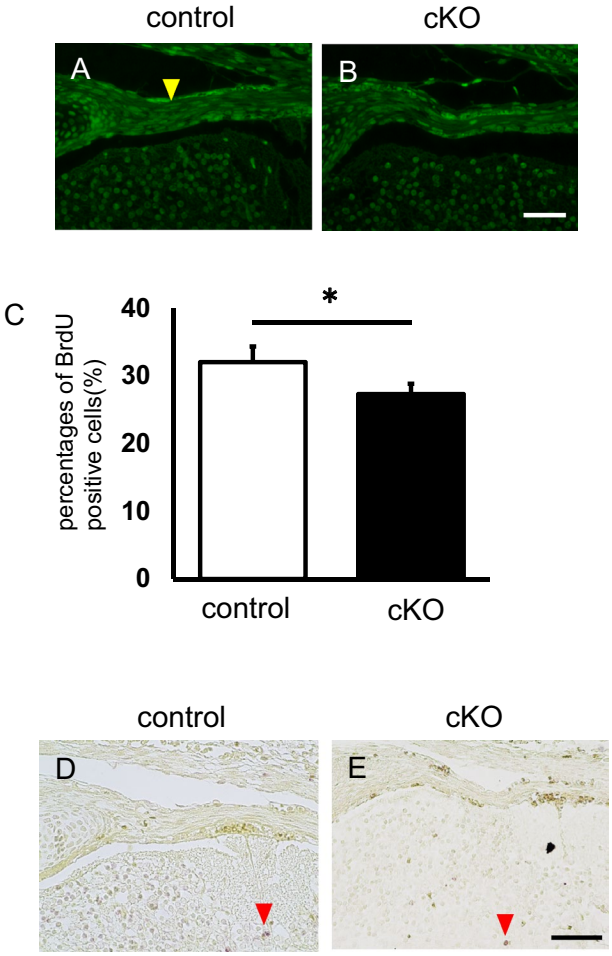

Fig. 5. G9a deletion inhibits proliferation but does not affect apoptosis in developing tendons. BrdU was injected at E16.5 and recovered at E17.5. BrdU incorporation was assessed in the vertebral tenocytes of control (**A**, *G9a*$^{fl/+}$; *Sox9*$^{Cre/+}$) and *G9a* cKO mice (**B**, *G9a*$^{fl/fl}$; *Sox9*$^{Cre/+}$) by using an anti-BrdU antibody (control n = 2; cKO n = 2). Immunofluorescence images of BrdU-labeled cells are shown. The yellow arrowheads indicate strongly positive cells. Bar = 50 µm. (**C**) Comparison of the percentages of BrdU-positive cells (n = 3). We counted 60–64 cells/section and three independent sections were analyzed (*$p < 0.05$, t-test). (**D** and **E**) TUNEL staining in vertebral tenocytes of control (**D**, *G9a*$^{fl/+}$; *Sox9*$^{Cre/+}$) and *G9a* cKO (**E**, *G9a*$^{fl/fl}$; *Sox9*$^{Cre/+}$) mouse embryos at E16.5. Red arrowheads indicate apoptotic nuclei. Bar = 50 µm.

Expression levels of tendon markers decreased in the developing tendons in *G9a* cKO mice

To examine the expression of the molecular markers of tenocyte differentiation, we performed immunostaining for type I collagen, which is the major component of the tendon extracellular matrix. At E17.5, type I collagen was expressed in the tendon tissue of control mice (Fig. 6A,C), whereas its signal was lower in the vertebral tendon tissue of *G9a* cKO mice (Fig. 6B,D). ISH experiments also showed that *Col1a1* mRNA levels were reduced in the tenocytes of G9a mutant embryos by E16.5, in comparison with the levels in control embryos (Fig. 6E–H). We also examined the expression of *Tnmd* and *Scx*, markers of tendon differentiation. *Tnmd* mRNA levels in the tenocytes of G9a-deleted embryos by E16.5 were also lower than those in control embryos (Fig. 6I–P). WISH experiments also showed a reduction in *Tnmd* mRNA levels in G9a-deleted limbs at E15.5 (Fig. 6S, T). ISH experiments showed that the numbers of cells expressing *Scx* mRNA seem to be lower in *G9a* cKO mice, however, its intensity in the tenocytes looks similar between *G9a* cKO and control embryos (Fig. 6Q,R). By q-PCR experiments, we found that mRNA levels of *Col1a1, Tnmd, and Scx* were suppressed in hindlimb tendon tissue in *G9a* cKO mice at E17.5 (Supplemental Fig. 3). We also checked testis-specific genes, which were shown to be activated in *G9a* KO embryos[10], and found that their expressions were not activated in *G9a* cKO tendons (Supplemental Fig. 4). Thus, the expression of tendon differentiation markers was decreased in *G9a* cKO mice.

Overexpression of G9a resulted in enhancement of *Tnmd* and *col1a1* expression in tenocytes in vitro

Previously we showed the expression levels of tendon-related genes *Tnmd*, *Col1a1*, *and Scx* were decreased in G9a deleted tenocytes in vitro. From the results of both in vivo and in vitro studies, we have assumed that G9a is involved in the activation of those gene expressions. To test this assumption, we performed overexpression

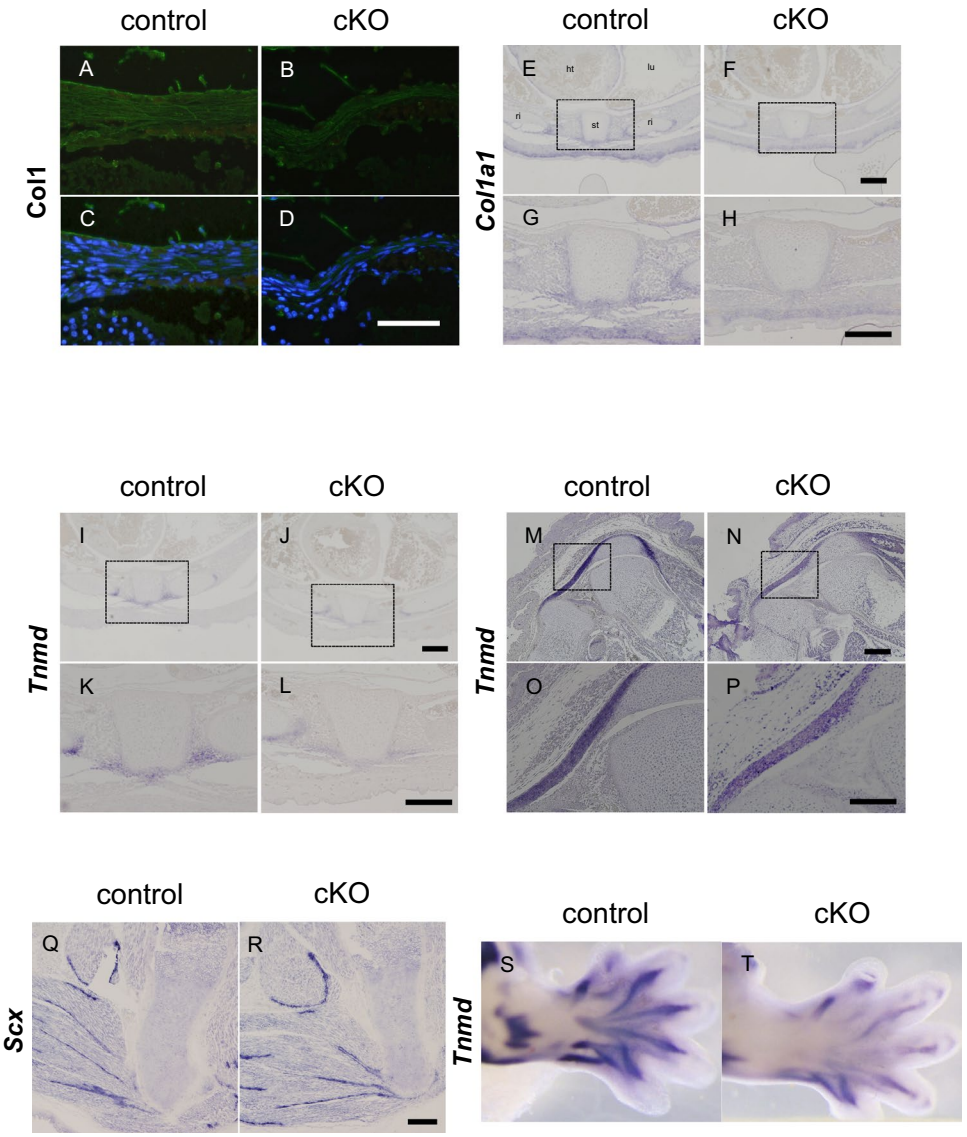

Fig. 6. Decreased expressions of tendon markers in developing tendons in *G9a* cKO mice. (**A**–**D**) Immunohistochemical analysis of type I collagen in the vertebral tendon tissue of control (**A** and **C**, $G9a^{+/+}$; $Sox9^{Cre/+}$) and *G9a* cKO mice (**B** and **D**, $G9a^{fl/fl}$; $Sox9^{Cre/+}$) at E17.5 (control n = 3; cKO n = 3). Immunofluorescent images of staining with anti-Col1 antibody (**A** and **B**) (*green*), and merged images of anti-Col1 immunostaining and nuclear staining with DAPI (*blue*) (**C** and **D**). Bar = 50 µm. (**E**–**P**) In situ hybridization (ISH) on transverse sections of the trunk (**E**–**L**) and sagittal sections of the hindlimb (**M**–**P**) at E16.5 (control n = 3; cKO n = 3). Tissue sections from control (**E**, **G**, **I**, **K**, **M**, **O**, and **Q**, $G9a^{+/+}$; $Sox9^{Cre/+}$) and *G9a* cKO (**F**, **H**, **J**, **L**, **N**, **P**, and **R**, $G9a^{fl/fl}$; $Sox9^{Cre/+}$) embryos were analyzed using antisense RNA probes for tendon markers, collagen type I alpha 1 chain (*Col1a1*), tenomodulin (*Tnmd*), and screlaxis (*Scx*) mRNA. Ht, heart; lu, lung; st, sternum; ri, rib. Bar = 100 µm (**E**–**P**), 200 µm (**Q** and **R**). Whole-mount ISH of *Tnmd* in forelimbs from control (**S**, $G9a^{+/+}$; $Sox9^{Cre/+}$) and G9a*G9a* cKO mice (**T**, $G9a^{fl/fl}$; $Sox9^{Cre/+}$) was performed at E15.5 (control n = 3; cKO n = 3).

experiment of G9a in tenocytes. Adenovirus expression of G9a in tenocytes resulted in increase of *Tnmd*, *Col1a1,* and *Six2* gene expressions, whereas *Scx* expression was suppressed (Fig. 7A). Western blot analysis showed that protein levels of Tnmd and Col1a1 were also increased (Fig. 7B and Supplemental Fig. 5).

We confirmed that H3K9me2 level was increased along with G9a overexpression (Fig. 7B). Cell proliferation assay showed that slight increase of proliferation in G9a over-expressed cells on day 1 (Fig. 7C). Expression of a cell cycle negative regulator, *p21*, was suppressed in those cells (Fig. 7A). These results suggest that G9a activates some of tendon-related genes in tenocytes independent of H3K9me2-mediated gene suppression.

Discussion

In the present study, we showed that conditional deletion of the *G9a* gene resulted in inhibition of cell growth and a decrease in tendon marker expression, leading to tendon hypoplasia during development.

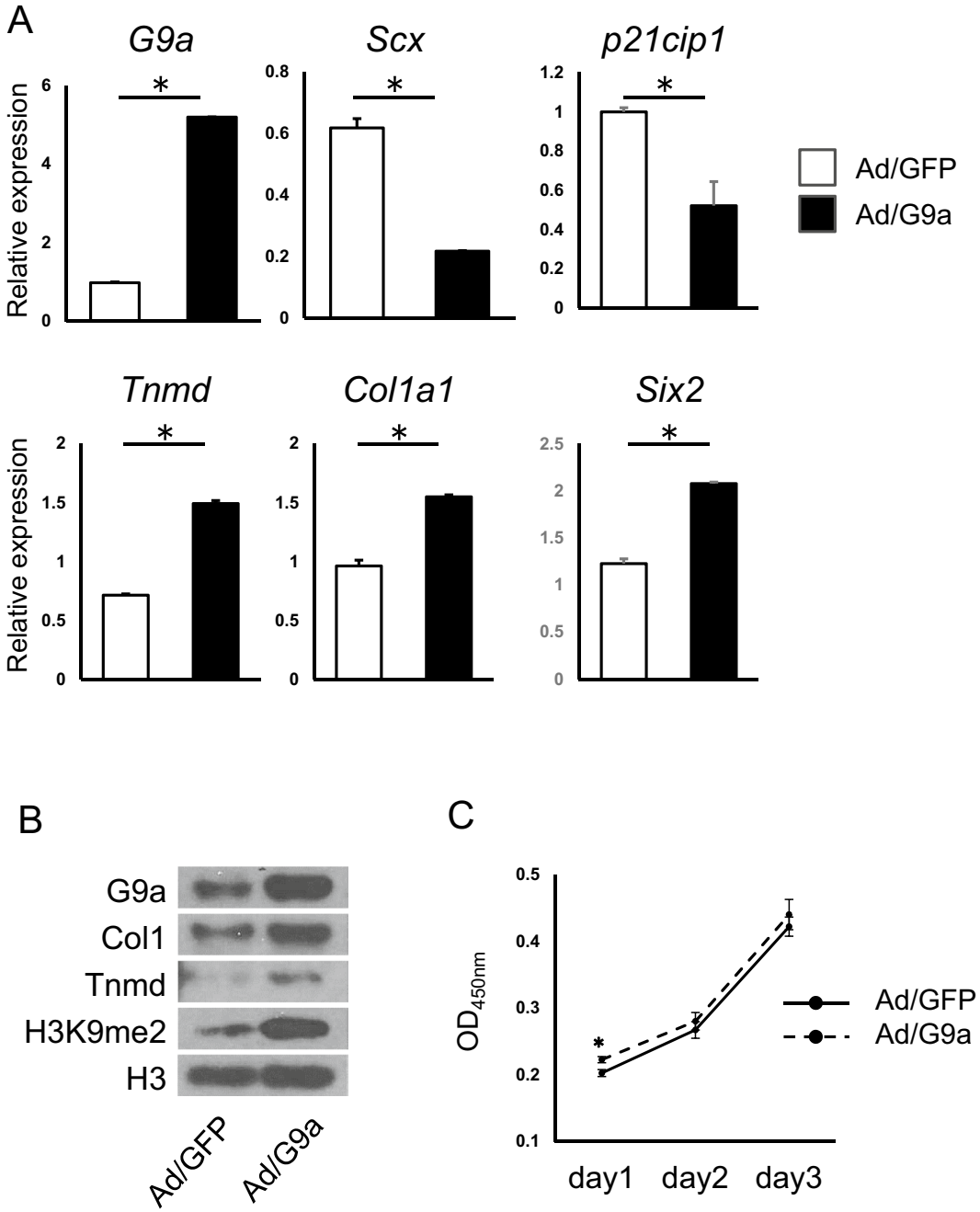

Fig. 7. Overexpression of G9a resulted in enhancement of tendon marker expressions in tenocytes in vitro. Primary tenocytes were infected with adenoviruses expressing G9a (Ad/G9a) or GFP (Ad/GFP). (**A**) Expression of tendon marker genes at day 4 after the adenovirus infection. Gene expressions of *G9a*, *Scx*, *p21cip1*, *Tnmd, Col1a1*, and *Six2* were shown. Representative results of four independent experiments are shown (*$p < 0.05$, t-test). (**B**) Proteins were extracted at day 4 after adenovirus infection. Protein levels of G9a, COL1A1, Tnmd, and H3K9me2 are shown. Histone H3 protein is served as an internal loading control. Representative results of three independent experiments are shown. (**C**) Measurement of cell proliferation was performed at day1, 2 and 3 after the adenovirus infection. Representative results of two independent experiments are shown (*$p < 0.05$, t-test).

During tendon development, tendon progenitors arise from the sclerotome, lateral plate mesoderm, and neural crest[24,37]. These progenitor cells migrate and settle in the prospective region, giving rise to the skeletal primordia[38]. Sox9 is expressed in the mesenchymal condensation of skeletal primordia and gives rise to cartilage, bone, and tendon later in the development[23–25]. In this study, we confirmed LacZ expression in vertebral tendon tissue, indicating the functionality of *Sox9-Cre* in tendon progenitor cells (Fig. 1). Previously we showed that *G9a* is expressed in embryonic tendon progenitor cells[21]. The results of the present study suggest that G9a

deletion in *Sox9*-expressing tendon progenitor cells inhibited cell proliferation and differentiation, leading to tendon hypoplasia.

Our findings showed that *G9a* cKO mice exhibit suppressed tenocyte proliferation during development. G9a has been reported to be overexpressed in a number of cancers[39–41], and the loss of G9a has been shown to inhibit cell proliferation in various cells[42,43]. Previous studies have reported that G9a represses the expression of negative regulators of the cell cycle, such as $p21^{Cip1/Waf1}$ (p21), in a methyltransferase activity-dependent manner in several cell types[44–46]. We previously showed that the proliferation of G9a-null tenocytes was significantly decreased and the *p21* gene was upregulated in vitro[21]. In this study, we found that overexpression of G9a resulted in down-regulation of *p21* gene and slight increase of cell proliferation in tenocytes. Therefore, G9a may promote cell-cycle progression by transcriptionally repressing p21 expression in tenocytes. G9a represses p21 by mediating H3K9me2 marks, whereas it regulates the E2F1 target genes, CyclinD1 and DHFR, leading to cellular proliferation in myoblasts[46]. Thus, one possible mechanism for the inhibition of tenocyte proliferation in *G9a* cKO mice is the regulation of cell-cycle modulators by G9a.

Our data also showed that *Tnmd* expression was suppressed in the developing tendon of *G9a* cKO mice. A previous study reported that cell growth is suppressed in *Tnmd*-null mice[47]. Furthermore, the loss of *Tnmd* has been shown to result in the suppression of mouse tendon stem/progenitor cells (mTSPCs)[48]. *Tnmd*-knockout mTSPCs showed significantly decreased expression of the *Cyclin D1* gene and increased *p53* mRNA expression. Furthermore, LacZ staining revealed that the number of senescent cells was increased in *Tnmd*-knockout TSPCs, although apoptosis was not affected. Our data also showed that tenocyte proliferation was inhibited and apoptosis did not change in the *G9a* cKO mice. Therefore, G9a may indirectly suppress cell growth through *Tnmd* expression.

G9a mediates methylation of H3K9me2, which is associated with the formation of transcriptionally inactive heterochromatin and gene silencing[49]. However, the expression of tendon markers such as type I collagen and Tnmd was suppressed in the developing tendons of *G9a* cKO mice, in accordance with our previous data in vitro[21]. Furthermore, G9a overexpression in tenocytes increased expressions of *Col1a1*, *Tnmd,* and *Six2*, although H3K9me2 level was increased. Thus, it suggests that G9a activates those tendon genes in tenocytes, independent of H3K9me2 mediated transcriptional repression. How does G9a activate those cell lineage-related genes? Several possibilities were proposed in other type of cells[13,14,18,50]. In erythroid cells, G9a recruits Mediator to the βmaj promoter of the β globin gene to activate its expression[18]. In prostate cancer cells and osteoblasts, G9a was recruited to endogenous Runx2 binding sites to activate Runx2 target genes[15,50]. In tenocytes, it was shown that promoters of *Tnmd* and *Six2* have Scx binding sites and their expressions are Scx-dependent[34]. Although G9a overexpression suppressed *Scx* expression, *Tnmd* and *Six2* expressions were increased in tenocytes, raising a possibility that G9a promotes Scx action in tenocytes. Another possibility could be that G9a recruits Mediator to the promoter of *Tnmd* and *Six2* genes in tenocytes, similar to the promoter of *β globin* gene in erythroid cells.

In contrast to tenocytes, other studies have reported that the suppression of G9a increases *Tnmd* and *Col1a1* expressions in various cells. In the *G9a*-KO testis and ovaries, *Tnmd* expression is upregulated[51]. *Col1a1* expression was increased in vascular smooth muscle, and liver cells[52,53]. Therefore, the effects of G9a deletion on *Tnmd* and *Col1a1* genes are likely context-and/or cell type-dependent. In the *G9a* KO E8.5 embryos, testis-specific genes are upregulated, in which G9a-guided DNA methylation represses germline genes[10]. However, germline genes were not activated in tendons in *G9a* cKO mice (Supplemental Fig. 4), suggesting that suppression of germline genes by G9a-guided DNA methylation is cell type-dependent.

Our results suggest that in tendon development G9a activates tendon-related genes independent of H3K9me2 mediated transcriptional repression, and suppresses p21 expression through H3K9me2. Thus, G9a functions as a repressor or activator depending on its associating partners. Further studies are required to explore this switching mechanism in detail.

Sox9-expressing cells are known to contribute to chondrogenic cells[54], and *Sox9* and *Scx* double-positive progenitors reside in the chondrotendinous junction during development and later become tenocytes and chondrocytes[55,56]. Since tendon progenitors and chondrocytes mutually interact during development, the repression of proliferation of tendon progenitors may be attributable to an indirect mechanism involving G9a deletion in chondrogenic cells. Since *Sox9-Cre* influences both tendon progenitors and chondrocytes, the findings for our cKO mice could not distinguish the effects on tenocytes from the indirect effects mediated through chondrogenesis, which is a limitation of our study using *Sox9-Cre*-expressing cKO mice.

In conclusion, our data indicate that G9a plays an essential role in tendon development. These findings suggest that G9a regulates cell growth and gene expression via epigenetic changes during tendon development. These results offer insights into the mechanism underlying tendon development and repair, suggesting potential approaches targeting tendon-related disorders.

Materials and methods

Animals

All animal experiments were approved by the Institutional Animal Care Committee, and the Recombination Experiment and Biosafety Committee of Tsurumi University School of Dental Medicine. Mice were cared for in accordance with the National Institutes of Health Guide for the Care and Use of Laboratory Animals and our institutional guidelines. All animal experiments in this study were done in accordance with ARRIVE guidelines.

To generate $G9a^{fl/fl}$ ($Ehmt2^{tm2Yshk}$) mice, G9a deleted in ES cells (TT2 cell line) were injected into ICR mouse embryos[51]. $G9a^{fl/+}$ mice were sequentially backcrossed with the C57BL/6 background mice, and offsprings later than F15 generation were used for further studies. $Sox9^{Cre/+}$($Sox9^{tm3(cre)Crm}$) mice, which were generously given by Prof. Haruhiko Akiyama[24], were intercrossed with $G9a^{fl/+}$ mice to generate a conditional mutant mouse line lacking *G9a*, *G9a*-cKO (Sox9-specific G9a gene deletion: $G9a^{fl/fl}$; $Sox9^{Cre/+}$) mice. $G9a^{fl/+}$ mice were served as

control. Polymerase chain reaction genotyping of *G9a* cKO mice was performed using the following primer pairs: mGE28R (GCTCCAGGGCGATGGCCTCCGCTGAATGC) and mGI27-2F (CGGGACAGGGTTTCTCTGTGT AGTCC) for wild-type *G9* allele detection, mGE28R and G3 (GGGCCAGCTCATTCCTCCACTC) for floxed *G9a* allele detection, and Sox9-Cre-F1 (TCCAATTTACTGACCGTACACCAA) and Sox9-Cre-R1 (CCTGAT CCTGGCAATTTCGGCTA) for $Sox9^{Cre}$ allele detection. R26R mutant mice carrying a *loxP* flanked neo cassette upstream of a β-galactosidase (lacZ) sequence were obtained from the Jackson Laboratory and were intercrossed with $Sox9^{Cre/+}$ mice to generate $Sox9^{Cre/+}$; *R26R* mice to detect cells derived from *Sox9*-expressing cells.

Antibodies

The following antibodies were used in this study: anti-H3K9me2 (CMA307; mouse monoclonal, prepared by H. Kimura[57]); anti-G9a (PP-A8620A-00, mouse monoclonal; Perseus Proteomics, Tokyo, Japan); anti-type I collagen (2150-1410, rabbit polyclonal; AbD Serotec, Oxford, UK); anti-tenomodulin (bs-7525R, rabbit polyclonal; Bioss Inc., MA); anti-BrdU (111703760011, mouse monoclonal; Roche, IN); anti-PCNA (2586, mouse monoclonal; Cell Signaling Technology, Danvers, MA); anti-H3 (MABI0301, mouse monoclonal; MAB Institute Inc., Nagano, Japan); anti-mouse IgG-HRP (1858413, goat rabbit polyclonal; Pierce, IL); anti-rabbit IgG-HRP (1858415, goat rabbit polyclonal; Pierce) and anti-mouse IgG (H + L)-Alexa488 (A11001, goat polyclonal; Invitrogen, Carlsbad, CA). The anti-H3K9me2 antibody is specific for histone H3 dimethyl Lys9, which has no cross-reactivity with other histone modifications including H3K27me2 evaluated by ELISA[57]. By immunofluorescent analysis using this antibody, we showed that levels of H3K9me2 in the G9a-deleted tissues were significantly low, suggesting the specificity of this antibody in immunofluorescence (see Kamiunten et al.[36] and results of Fig. 2 in this study).

LacZ activity staining

Staining for LacZ activity was performed as described previously[58]. Briefly, dissected tissues were fixed with 0.25% glutaraldehyde in phosphate-buffered saline (PBS) for 1 h at room temperature, treated overnight with 20% sucrose in PBS at 4 °C, and embedded in Tissue-Tek® OCT compound (Sakura Finetek Japan, Tokyo, Japan). Frozen sections (12-μm sections) were prepared. Before staining, the sections were treated with fixation solution (0.2% glutaraldehyde, 5 mM EGTA, 2 mM $MgCl_2$) at 4 °C for 5 min. After washing (phosphate buffer containing 2 mM $MgCl_2$, 0.01% sodium deoxycholate, and 0.02% Nonidet P-40), the sections were incubated with X-gal staining solution (5 mM potassium ferrocyanide, 5 mM potassium ferricyanide, and 1 mg/mL X-gal) for 6 h at room temperature.

Immunohistochemistry

Immunohistochemical analyses were performed using primary antibodies against G9a, H3K9me2, and ColI. At embryonic day 16.5 (E16.5), embryos were fixed with 4% paraformaldehyde (PFA) in PBS for 24 h. PFA-fixed tissue was embedded in paraffin, and 5-μm sections were prepared. After deparaffinization, sections were heated in a microwave in 10 mM citric acid buffer (pH 6) for 20 min. During microwaving, the temperature of the buffer was maintained at 90 °C. Then, the sections were treated with blocking solution in goat serum and incubated overnight at 4 °C with one of the following primary antibodies: anti-H3K9me2 (1:100), anti-G9a (1:400), anti-PCNA (1:400), and anti-Col1 (1:400). After washing, the sections were incubated with secondary antibodies conjugated to Alexa Fluor 488 (1:1000) and DAPI (1:10, CS-2010-06; Cosmo Bio, Tokyo, Japan). Fluorescent images were acquired using a Keyense BZ-9000 microscope. The percentages of G9a-positive and H3K9me2-positive cells were calculated as the number of positive cells/number of cells with DAPI-stained nuclei. These values were compared between the control and *G9a* cKO mice.

In situ hybridization and whole-mount in situ hybridization

In situ hybridization (ISH) of transverse sections and whole-mount in situ hybridization (WISH) were performed on mouse embryos collected at E15.5, as described previously[59]. RNA probes for the following regions were used for ISH studies: *Col1a1* (AK159285; 4446-4759), *Scx* (NM_198885; 415-1128), and *Tnmd* (NM_022322; 654-1299).

Bromodeoxyuridine labeling experiment

Bromodeoxyuridine (BrdU) labeling was performed as described previously[60]. E16.5 pregnant mice were subcutaneously injected with BrdU at a dose of 50 μg/g body weight in 0.9% NaCl. The mice were euthanized by manual cervical dislocation 24 h after injection and dissected to obtain the tendon tissues. Then, the tissues were fixed in PFA at 4 ℃ overnight, embedded in paraffin, and cut into 5-μm sections. After deparaffinization, the sections were treated with 2 N hydrochloric acid (HCl) for 90 min at 37 ℃ to denature DNA and then neutralized with 0.1 M boric acid for 5 min. The prepared sections were reacted with anti-BrdU monoclonal antibody diluted 1/400 in CanGetSignal® immunostain (TOYOBO, Osaka, Japan) overnight at 4 °C. After washing, the sections were incubated with secondary antibodies conjugated to Alexa Fluor 488 (1:1000). Fluorescent images were acquired using a Keyense BZ-9000 microscope. The percentage of BrdU-positive cells was calculated as the number of BrdU-positive cells divided by the number of cells counted using DAPI staining.

Cell culture

Primary tenocytes were isolated from the tail tendons of 12-week-old mice by collagen gel culture as previously described[21]. The cells were then plated at 2×10^4 cells/cm^2 in alpha minimal essential medium (alpha-MEM) supplemented with 10% fetal bovine serum (FBS) in a humidified atmosphere of 5% CO2 and 95% air. Subsequently, the cells were incubated for the indicated period of time with a change of medium every 2 days.

Preparation of adenovirus vectors and their infection into tenocytes
The production of adenovirus was performed as described previously[61]. according to the manufacturer's protocol (ViraPower Adenoviral Expression System; Thermo Fisher Scientific). An adenovirus vector expressing enhanced green fluorescent protein (EGFP) (Ad/GFP), which contains CAG-IRES-EGFP, was prepared as described[61]. Another adenovirus vector expressing G9a (Ad/G9a) was constructed as described previously[62]. Infection of adenovirus was performed on the day of plating at multiplicity of infection (MOI) 50.

Measurement of cell proliferation
Primary tenocytes infected with Ad/GFP or Ad/G9a at a MOI 50 were seeded at 1.6×10^4 cells/well into 48 well plates. A solution from the Cell Counting Kit-8 (CCK-8) (Dojin Chemistry, Kumamoto, Japan) was added 20 µL per well at 1, 2, and 3 days after plating and incubated for 1 h. Absorbance (450 nm) was measured using a microplate reader (Molecular device, CA).

Western blot analysis
Western blot analysis was performed as described[21]. Briefly, the proteins were extracted and lysed in 1 × SDS sample buffer (New England Biolabs, Beverly, MA) in which a complete protease inhibitor mixture tablet (Roche Diagnostics, Indianapolis, IN) was dissolved. The lysed proteins were separated on 10% Super Sep™ Ace SDS–PAGE gel (Wako Pure Chemicals, Osaka, Japan) and electro-transferred to PVDF membranes (PALL, Ann Arbor, MI). Primary antibodies [G9a (1:1,000), Col1 (1:1,000), Tnmd (1:1,000), H3K9me2 (1:1000), H3 (1:1,000)] were used in Can Get Signal solution 1 (Toyobo, Osaka, Japan) at room temperature (RT) for 1 h. Secondary antibodies, HRP-conjugated goat anti-rabbit IgG and HRP-conjugated goat anti-mouse IgG, were used at a dilution of 1:5000 in Can Get Signal solution 2 (Toyobo) and hybridized to membranes at RT for 1 h. Immunoreactive bands were detected by chemiluminescence using Western Lightning ECL Pro (Perkin-Elmer, Waltham, MA).

Reverse transcription and real-time PCR
RNA was isolated using an RNeasy Mini Kit (Qiagen, Hilden, Germany) according to the manufacturer's instructions. RNA was reverse transcribed using oligo-dT primers and reverse transcriptase (Superscript III; Invitrogen) to synthesize cDNA. After cDNA synthesis, qPCR was performed as previously described[61]. Three or more independent cultures were subjected to qPCR and representative results are shown. The primer sequences used for each PCR experiment are listed in Table 1.

TUNEL assay

The TUNEL assay was conducted using an In Situ Cell Death Detection Kit according to the manufacturer's instructions (Roche, Penzberg, Germany). Deparaffined sections were treated with proteinase K (1 µg/mL in 10 mM Tris/HCl, pH 7.5) for 40 min at 37 °C. The sections were then rinsed with PBS. Next, the sections were incubated with TUNEL reaction mixture for 1 h at 37 °C and then rinsed with PBS. The sections were further incubated with Converter AP Solution for 30 min at 37 °C and then rinsed with PBS. The sections were stained by incubation with 0.2 mg/mL naphthol AS-MX phosphate (Sigma), 0.4 mg/mL fast red BB salt (Sigma), 0.5% NN-dimethylformamide, 2 mM $MgCl_2$, and 2 mM levamisole in 100 mM Tris-maleic acid (pH 9.2) for 15 min at room temperature.

Statistical analysis

Statistical analysis was performed using an unpaired Student's *t* test. *P*-values < 0.05 were considered to be statistically significant.

	Forward primer (5′-)	Reverse primer (5′-)
Gapdh	GCCAAACGGGTCATCATCTC	GTCATGAGCCCTTCCACAAT
G9a	CTCTACCGGACTGCCAAGAT	CTCGGCATCAGAGATCAGC
Scx	CACCCAGCCCAAACAGATCTGCA	AGTGGCATCACCTCTTGGCTGCT
Tnmd	TCCCGCAAGTGAAGGTGGAGAAGA	AGTAAAGGTTCACAGACACGGCGG
Col1a1	GTCTGACTGGTCCCATTGGT	ATCACCAGGTTCACCTTTCG
Six2	ACCACCACGCAAGTCAGCAA	CGACTTGCCACTGCCATTGA
p21Cip1	TTGCACTCTGGTGTCTGAGC	TGCGCTTGGAGTGATAGAAA
Brdt	GGTGGACGCCGTGAAACTAAA	GGGCCATAACAACAATGTCATCT
Ptpn20	TCACCCAGGAAGGTTAGAGGA	GAGTTGCGGAGATTCAGGTTAC

Table 1. Primer lists for qPCR.

Data availability

The data that support the findings are available in the methods section.

Received: 24 March 2024; Accepted: 29 August 2024
Published online: 05 September 2024

References

1. Mozzetta, C., Boyarchuk, E., Pontis, J. & Ait-Si-Ali, S. Sound of silence: The properties and functions of repressive Lys methyltransferases. *Nat. Rev. Mol. Cell Biol.* **16**, 499–513 (2015).
2. Greer, E. L. & Shi, Y. Histone methylation: A dynamic mark in health, disease and inheritance. *Nat. Rev. Genet.* **13**, 343–357 (2012).
3. Padeken, J., Methot, S. P. & Gasser, S. M. Establishment of H3K9-methylated heterochromatin and its functions in tissue differentiation and maintenance. *Nat. Rev. Mol. Cell Biol.* **23**, 623–640 (2022).
4. Volkel, P. & Angrand, P. O. The control of histone lysine methylation in epigenetic regulation. *Biochimie* **89**, 1–20 (2007).
5. Shinkai, Y. & Tachibana, M. H3K9 methyltransferase G9a and the related molecule GLP. *Genes Dev.* **25**, 781–788 (2011).
6. Feldman, N. *et al.* G9a-mediated irreversible epigenetic inactivation of Oct-3/4 during early embryogenesis. *Nat. Cell Biol.* **8**, 188–194 (2006).
7. Roopra, A., Qazi, R., Schoenike, B., Daley, T. J. & Morrison, J. F. Localized domains of G9a-mediated histone methylation are required for silencing of neuronal genes. *Mol. Cell* **14**, 727–738 (2004).
8. Gyory, I., Wu, J., Fejer, G., Seto, E. & Wright, K. L. PRDI-BF1 recruits the histone H3 methyltransferase G9a in transcriptional silencing. *Nat. Immunol.* **5**, 299–308 (2004).
9. Tachibana, M. *et al.* G9a histone methyltransferase plays a dominant role in euchromatic histone H3 lysine 9 methylation and is essential for early embryogenesis. *Genes Dev.* **16**, 1779–1791 (2002).
10. Auclair, G. *et al.* EHMT2 directs DNA methylation for efficient gene silencing in mouse embryos. *Genome Res.* **26**, 192–202 (2016).
11. AuYeung, W. K. *et al.* Histone H3K9 methyltransferase G9a in oocytes is essential for preimplantation development but dispensable for CG methylation protection. *Cell Rep.* **27**, 282–293 (2019).
12. Ling, B. M. *et al.* Lysine methyltransferase G9a methylates the transcription factor MyoD and regulates skeletal muscle differentiation. *Proc. Natl. Acad. Sci. U. S. A.* **109**, 841–846 (2012).
13. Lee, D. Y., Northrop, J. P., Kuo, M. H. & Stallcup, M. R. Histone H3 lysine 9 methyltransferase G9a is a transcriptional coactivator for nuclear receptors. *J. Biol. Chem.* **281**, 8476–8485 (2006).
14. Bittencourt, D. *et al.* G9a functions as a molecular scaffold for assembly of transcriptional coactivators on a subset of glucocorticoid receptor target genes. *Proc. Natl. Acad. Sci. U. S. A.* **109**, 19673–19678 (2012).
15. Ideno, H. *et al.* G9a is involved in the regulation of cranial bone formation through activation of Runx2 function during development. *Bone* **137**, 115332 (2020).
16. Poulard, C. *et al.* A post-translational modification switch controls coactivator function of histone methyltransferases G9a and GLP. *EMBO Rep.* **18**, 1442–1459 (2017).
17. Zhang, X. *et al.* G9a-mediated methylation of ERα links the PHF20/MOF histone acetyltransferase complex to hormonal gene expression. *Nat. Commun.* **7**, 10810 (2016).
18. Chaturvedi, C. P. *et al.* Dual role for the methyltransferase G9a in the maintenance of beta-globin gene transcription in adult erythroid cells. *Proc. Natl. Acad. Sci. U. S. A.* **106**, 18303–18308 (2009).
19. Ideno, H. *et al.* Predominant expression of H3K9 methyltransferases in prehypertrophic and hypertrophic chondrocytes during mouse growth plate cartilage development. *Gene Expr. Patt.* **13**, 84–90 (2013).
20. Kamiunten, T. *et al.* Coordinated expression of H3K9 histone methyltransferases during tooth development in mice. *Histochem. Cell Biol.* **143**, 259–266 (2015).
21. Wada, S. *et al.* H3K9MTase G9a is essential for the differentiation and growth of tenocytes in vitro. *Histochem. Cell Biol.* **144**, 13–20 (2015).
22. He, P. *et al.* Comparison of tendon development versus tendon healing and regeneration. *Front. Cell Dev. Biol.* **10**, 821667 (2022).
23. Asou, Y. *et al.* Coordinated expression of scleraxis and Sox9 genes during embryonic development of tendons and cartilage. *J. Orthop. Res.* **20**, 827–833 (2002).
24. Akiyama, H. *et al.* Osteo-chondroprogenitor cells are derived from Sox9 expressing precursors. *Proc. Natl. Acad. Sci. U. S. A.* **102**, 14665–14670 (2005).
25. Soeda, T. *et al.* Sox9-expressing precursors are the cellular origin of the cruciate ligament of the knee joint and the limb tendons. *Genesis* **48**, 635–644 (2010).
26. Spanoudes, K., Gaspar, D., Pandit, A. & Zeugolis, D. I. The biophysical, biochemical, and biological toolbox for tenogenic phenotype maintenance in vitro. *Trends Biotechnol.* **32**, 474–482 (2014).
27. Riley, G. Tendinopathy-from basic science to treatment. *Nat. Clin. Pract. Rheumatol.* **4**, 82–89 (2008).
28. Huang, A. H., Lu, H. H. & Schweitzer, R. Molecular regulation of tendon cell fate during development. *J. Orthop. Res.* **33**, 800–812 (2015).
29. Murchison, N. D. *et al.* Regulation of tendon differentiation by scleraxis distinguishes force-transmitting tendons from muscle-anchoring tendons. *Development* **134**, 2697–2708 (2007).
30. Ito, Y. *et al.* The Mohawk homeobox gene is a critical regulator of tendon differentiation. *Proc. Natl. Acad. Sci. U. S. A.* **107**, 10538–10542 (2010).
31. Liu, W. *et al.* The atypical homeodomain transcription factor Mohawk controls tendon morphogenesis. *Mol. Cell. Biol.* **30**, 4797–4807 (2010).
32. Lejard, V. *et al.* EGR1 and EGR2 involvement in vertebrate tendon differentiation. *J. Biol. Chem.* **286**, 5855–5867 (2011).
33. Guerquin, M. J. *et al.* Transcription factor EGR1 directs tendon differentiation and promotes tendon repair. *J. Clin. Invest.* **123**, 3564–3576 (2013).
34. Liu, H., Xu, J., Lan, Y., Lim, H. W. & Jiang, R. The scleraxis transcription factor directly regulates multiple distinct molecular and cellular processes during early tendon cell differentiation. *Front. Cell Dev. Biol.* **9**, 654397 (2021).
35. Pal, D. *et al.* Ezh2 Is essential for patterning of multiple musculoskeletal tissues but dispensable for tendon differentiation. *Stem Cells Dev.* **30**, 601–609 (2021).
36. Kamiunten, T. *et al.* Essential roles of G9a in cell proliferation and differentiation during tooth development. *Exp. Cell Res.* **357**, 202–210 (2017).
37. Brent, A. E., Schweitzer, R. & Tabin, C. J. A somitic compartment of tendon progenitors. *Cell* **113**, 235–248 (2003).
38. Kardon, G. Muscle and tendon morphogenesis in the avian hind limb. *Development* **125**, 4019–4032 (1998).
39. Casciello, F., Windloch, K., Gannon, F. & Lee, J. S. Functional role of G9a histone methyltransferase in cancer. *Front. Immunol.* **6**, 487 (2015).
40. Lehnertz, B. *et al.* The methyltransferase G9a regulates HoxA9-dependent transcription in AML. *Genes Dev.* **28**, 317–327 (2014).
41. Dong, C. *et al.* G9a interacts with Snail and is critical for Snail-mediated E-cadherin repression in human breast cancer. *J. Clin. Invest.* **122**, 1469–1486 (2012).

42. Ueda, J. *et al.* The hypoxia-inducible epigenetic regulators Jmjd1a and G9a provide a mechanistic link between angiogenesis and tumor growth. *Mol. Cell. Biol.* **34**, 3702–3720 (2014).
43. Ding, J. *et al.* The histone H3 methyltransferase G9A epigenetically activates the serine-glycine synthesis pathway to sustain cancer cell survival and proliferation. *Cell Metab.* **18**, 896–907 (2013).
44. Nishio, H. & Walsh, M. J. CCAAT displacement protein/cut homolog recruits G9a histone lysine methyltransferase to repress transcription. *Proc. Natl. Acad. Sci. U. S. A.* **101**, 11257–11262 (2004).
45. Kim, J. K., Esteve, P. O., Jacobsen, S. E. & Pradhan, S. UHRF1 binds G9a and participates in p21 transcriptional regulation in mammalian cells. *Nucleic Acids Res.* **37**, 493–505 (2009).
46. Rao, V. K. *et al.* G9a promotes proliferation and inhibits cell cycle exit during myogenic differentiation. *Nucleic Acids Res.* **44**, 8129–8143 (2016).
47. Docheva, D., Hunziker, E. B., Fassler, R. & Brandau, O. Tenomodulin is necessary for tenocyte proliferation and tendon maturation. *Mol. Cell. Biol.* **25**, 699–705 (2005).
48. Alberton, P. *et al.* Loss of tenomodulin results in reduced self-renewal and augmented senescence of tendon stem/progenitor cells. *Stem Cells Dev.* **24**, 597–609 (2015).
49. Tachibana, M., Sugimoto, K., Fukushima, T. & Shinkai, Y. Set domain-containing protein, G9a, is a novel lysine-preferring mammalian histone methyltransferase with hyperactivity and specific selectivity to lysines 9 and 27 of histone H3. *J. Biol. Chem.* **276**, 25309–25317 (2001).
50. Purcell, D. J. *et al.* Recruitment of coregulator G9a by Runx2 for selective enhancement or suppression of transcription. *J. Cell. Biochem.* **113**, 2406–2414 (2012).
51. Tachibana, M., Nozaki, M., Takeda, N. & Shinkai, Y. Functional dynamics of H3K9 methylation during meiotic prophase progression. *EMBO J.* **26**, 3346–3359 (2007).
52. Weng, X. *et al.* Sin3B mediates collagen type I gene repression by interferon gamma in vascular smooth muscle cells. *Biochem. Biophys. Res. Commun.* **447**, 263–270 (2014).
53. Lei, W. *et al.* Homocysteine induces collagen i expression by downregulating histone methyltransferase G9a. *PLoS One* **10**, e0130421 (2015).
54. Mori-Akiyama, Y., Akiyama, H., Rowitch, D. H. & de Crombrugghe, B. Sox9 is required for determination of the chondrogenic cell lineage in the cranial neural crest. *Proc. Natl. Acad. Sci. U. S. A.* **100**, 9360–9365 (2003).
55. Sugimoto, Y. *et al.* Scx+/Sox9+ progenitors contribute to the establishment of the junction between cartilage and tendon/ligament. *Development* **140**, 2280–2288 (2013).
56. Blitz, E., Sharir, A., Akiyama, H. & Zelzer, E. Tendon-bone attachment unit is formed modularly by a distinct pool of Scx- and Sox9-positive progenitors. *Development* **140**, 2680–2690 (2013).
57. Kimura, H., Hayashi-Takanaka, Y., Goto, Y., Takizawa, N. & Nozaki, N. The organization of histone H3 modifications as revealed by a panel of specific monoclonal antibodies. *Cell Struct. Funct.* **33**, 61–73 (2008).
58. Shimada, A., Komatsu, K., Nakashima, K., Poschl, E. & Nifuji, A. Improved methods for detection of beta-galactosidase (lacZ) activity in hard tissue. *Histochem. Cell Biol.* **137**, 841–847 (2012).
59. Nifuji, A. & Noda, M. Coordinated expression of noggin and bone morphogenetic proteins (BMPs) during early skeletogenesis and induction of noggin expression by BMP-7. *J. Bone Miner. Res.* **14**, 2057–2066 (1999).
60. Shimada, A., Shibata, T., Komatsu, K. & Nifuji, A. Improved methods for immunohistochemical detection of BrdU in hard tissue. *J. Immunol. Methods* **339**, 11–16 (2008).
61. Ideno, H. *et al.* Protein related to DAN and cerberus (PRDC) inhibits osteoblastic differentiation and its suppression promotes osteogenesis in vitro. *Exp. Cell Res.* **315**, 474–484 (2009).
62. Komatsu, K. *et al.* The G9a histone methyltransferase represses osteoclastogenesis and bone resorption by regulating NFATc1 function. *FASEB J.* **38**, e23779 (2024).

Acknowledgements

The authors would like to thank Prof. Haruhiko Akiyama and Dr Yoichi Shinkai for providing $Sox9^{Cre/+}$ mice and $G9a^{fl/+}$ mice, respectively.

Author contributions

S.W.: investigation, data analysis, manuscript writing; H.I.: investigation (in vitro experiments, in vivo experiments mouse handling including colony management); K.K. .: investigation; K.N.: provision of mechanistic insight; N.D.: provision of mechanistic insight; H.T.: provision of mechanistic insight; H.K.: methodology, resources; M.T.: methodology, resources; A. N.: conception and design, investigation, provision of mechanistic insight, manuscript writing.

Funding

This study was partially supported by JSPS KAKENHI (Grant Numbers: 16K11797, 21K10199 to S.W. 22390344, 15K15679, 18K09515, 20K09897, 21K09823 to A.N, 23K09158 to H.I).

Competing interests

The authors declare no competing interests.

Additional information

Supplementary Information The online version contains supplementary material available at https://doi.org/10.1038/s41598-024-71570-5.

Correspondence and requests for materials should be addressed to A.N.

Reprints and permissions information is available at www.nature.com/reprints.

Publisher's note Springer Nature remains neutral with regard to jurisdictional claims in published maps and institutional affiliations.

Open Access This article is licensed under a Creative Commons Attribution-NonCommercial-NoDerivatives 4.0 International License, which permits any non-commercial use, sharing, distribution and reproduction in any medium or format, as long as you give appropriate credit to the original author(s) and the source, provide a link to the Creative Commons licence, and indicate if you modified the licensed material. You do not have permission under this licence to share adapted material derived from this article or parts of it. The images or other third party material in this article are included in the article's Creative Commons licence, unless indicated otherwise in a credit line to the material. If material is not included in the article's Creative Commons licence and your intended use is not permitted by statutory regulation or exceeds the permitted use, you will need to obtain permission directly from the copyright holder. To view a copy of this licence, visit http://creativecommons.org/licenses/by-nc-nd/4.0/.

© The Author(s) 2024